Engineering Fracture Mechanics Vol. 38, No. 2/3, pp. 215–223, 1991
Printed in Great Britain.

0013-7944/91 $3.00 + 0.00

ANALYSIS OF CRACK–MICROCRACK INTERACTIONS AND DOUBLY KINKED CRACKS USING MULTIPLE SINGULAR POINTS ELEMENTS

B. K. DUTTA†, S. K. MAITI‡ and A. KAKODKAR†
†R.E.D., Bhabha Atomic Research Centre, Bombay-85, India
‡Indian Institute of Technology, Bombay-76, India

Abstract—The problems of crack–microcrack interactions and doubly kinked cracks have been analysed by the finite element method. In the first case the main crack tip SIF has been evaluated for different length of a collinear microcrack, which is located at a fixed distance. Through another case study the influence of a pair of stacked parallel microcracks on the SIF of a main crack has been studied by varying the spacing of the two microcracks. The third example deals with a doubly kinked crack. The SIF at the crack tip has been determined for various angles of the second kink. All the three examples have been studied employing the multiple point singularity elements and their degenerate forms. The finite element computations have been compared, whenever possible, with analytical solutions available in the literature. The accuracy of the finite element computations are good. This has been achieved using a relatively coarse discretisation.

INTRODUCTION

SINGULARITIES occur in close proximities at more than one point in many situations. The order of singularity is not always a constant, it changes from problem to problem. In the case of a straight line crack within a linear elastic solid there are singularities of a fixed order at the two end points. If the length of the crack is small the two singularities interact with each other. In the case of a kinked internal crack there are singularities at three points—one at the knee and the others at the two end points. The order of singularity at the two end points is of a square-root type, but the order of singularity at the knee is a variable one because it depends on the knee angle[1]. If lengths of both the kink and the main crack are small the three singularities will interact. The number of interacting singularities increases as the number of kinks increases. This is seen in the case of irregular or zig-zag cracks generated by stress corrosion cracking. If two or more straight cracks lie in close proximity, as in the case of a main crack surrounded by microcracks close to its tip, there will be as many interacting singularities as the neighbouring crack tips. In the case of three "V"-shaped cracks with different included angles located close by, there will be three interacting variable order singularities.

Analytical solution to some of these problems exist in the literature. These can also be studied by a routine finite element analysis using the conventional elements. This is not an attractive strategy because a large number of elements and nodes are required to obtain a reasonable degree of accuracy. We have demonstrated recently[2–4] that it is computationally advantageous to use special elements, which can model singularities of variable orders at more than one point. We have presented so far three elements, one 4-noded quadrilateral[2], a 3-noded triangle[3] and a 6-noded triangle[4]. The last one can be employed to handle up to three neighbouring singular points. In this paper we present case studies using all these elements on crack–microcrack interactions and doubly kinked cracks. Before taking up the case studies, the element formulations are first presented briefly in the next section. The finite element results have been compared, whenever possible, with the available analytical solutions.

ELEMENT FORMULATION

One point variable order singularity element

Figure 1 shows the coordinate system employed. The same type of coordinates have been used by Tracey and Cook[5] for developing their one-point variable order singularity element. Their

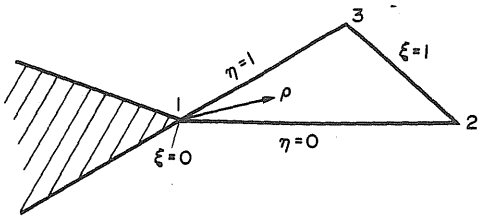

Fig. 1. Natural coordinate system for singular elements.

shape functions are given by

$$N_1 = 1 - \xi^\lambda$$
$$N_2 = \xi^\lambda(1 - \eta)$$
$$N_3 = \xi^\lambda \eta \tag{1}$$

where λ varies from 0 to 1 and the order of singularity is $\lambda - 1$. This element meets the rigid body mode and the interelement compatibility, but not the constant strain condition. The triangular coordinates (L_1, L_2, L_3), commonly used to derive shape functions for isoparametric triangular elements, are also shown in Fig. 1, are related to (ξ, η) by

$$\xi = 1 - L_1$$
$$\eta = L_3/(1 - L_1). \tag{2}$$

The shape functions for the Tracey and Cook[5] element in the triangular coordinates are

$$N_1 = 1 - (1 - L_1)^\lambda$$
$$N_2 = L_2(1 - L_1)^{\lambda - 1}$$
$$N_3 = L_3(1 - L_1)^{\lambda - 1}. \tag{3}$$

A careful examination of eq. (3) reveals that, if the ordinary shape functions are given by N_1, N_2 and N_3, then singular element shape functions may be written as

$$N_{1s} = 1 - (1 - N_1)^\lambda$$
$$N_{2s} = N_2(1 - N_1)^{\lambda - 1}$$
$$N_{3s} = N_3(1 - N_1)^{\lambda - 1}. \tag{4}$$

Equation (3) or (4) also implies that if there is a singularity at the i^{th} node, the shape function for the i^{th} node

$$N_{is} = 1 - (1 - N_i)\lambda \tag{5}$$

and the shape function for the j^{th} node

$$N_{js} = N_j(1 - N_i)^{\lambda - 1}. \tag{6}$$

A 3-noded two singular points finite element

In the case of a 3-noded triangular element, the ordinary shape functions are given by

$$N_1 = L_1; \quad N_2 = L_2 \quad \text{and} \quad N_3 = L_3. \tag{7}$$

Using the underlying logic behind eqs (4)–(6), we write the shape functions for a 3-noded element which displays the variable order singularities at its nodes 1 and 2 as

$$N_1 = C_1[\{1 - (1 - L_1)^{\lambda_1}\} + \{L_1(1 - L_2)^{\lambda_2 - 1}\}]$$
$$N_2 = C_2[\{1 - (1 - L_2)^{\lambda_2}\} + \{L_2(1 - L_1)^{\lambda_1 - 1}\}]$$
$$N_3 = C_3[\{L_3(1 - L_1)^{\lambda_1 - 1}\} + \{L_3(1 - L_2)^{\lambda_2 - 1}\}]. \tag{8}$$

The constants C_i are evaluated by requiring that $N_i = 1$ at the i^{th} node. This yields

$$C_1 = C_2 = C_3 = 0.5. \tag{9}$$

If the element displacement field is written using these shape functions, i.e.

$$u = \sum N_i u_i \quad \text{and} \quad v = \sum N_i v_i, \tag{10}$$

we obtain an element which has the stress/strain singularities at its nodes 1 and 2 of orders $\lambda_1 - 1$ and $\lambda_2 - 1$ respectively. The element meets the rigid body mode because $\Sigma N_i = 1$. The element is called here a two singular points triangular element (TSPT). To obtain an element with one variable order singular point, one needs to substitute $\lambda_2 = 1$ in eq. (8). We call such an element as degenerate two singular point element (DTSPT). If the DTSPT is used in association with the TSPT, the interelement compatibility is obtained.

A 6-noded multiple singular points finite element

Let us now consider the case of a 6-noded element for which ordinary shape functions are

$$N_1 = L_1(2L_1 - 1); \qquad N_2 = L_2(2L_2 - 1); \qquad N_3 = L_3(2L_3 - 1);$$

$$N_4 = 4L_1L_2; \qquad N_5 = 4L_2L_3; \qquad N_6 = 4L_3L_1. \tag{11}$$

Using again the underlying logic behind eqs (4)–(6), we can write the shape functions for a 6-noded element which displays singularity at node number 1 as follows:

$$\begin{aligned}
N_{1s} &= 1 - (1 - N_1)^\lambda \\
&= 1 - (1 - L_1)(2L_1 - 1))^\lambda \\
&= 1 - (1 - L_1)^\lambda (1 + 2L_1)^\lambda \\
N_{s2} &= L_2(2L_2 - 1)(1 - L_1)^{\lambda - 1}(1 + 2L_1)^{\lambda - 1} \\
N_{s3} &= L_3(2L_3 - 1)(1 - L_1)^{\lambda - 1}(1 + 2L_1)^{\lambda - 1} \\
N_{s4} &= 4L_1L_2(1 - L_1)^{\lambda - 1}(1 + 2L_1)^{\lambda - 1} \\
N_{s5} &= 4L_2L_3(1 - L_1)^{\lambda - 1}(1 + 2L_1)^{\lambda - 1} \\
N_{s6} &= 4L_3L_1(1 - L_1)^{\lambda - 1}(1 + 2L_1)^{\lambda - 1}.
\end{aligned} \tag{12}$$

The term $(1 + 2L_1)^\lambda$ does not have any singularity over the element. The singularity is therefore dependent only on the term $(1 - L_1)^\lambda$. This term also appears in the shape functions (eq. 3) of the Tracey and Cook[5] element.

If the element displacement field is written using this set of shape functions, we get a 6-noded triangle with singularity (at node no. 1) of order $\lambda - 1$. For $\lambda = 1$, we get back the shape functions for the 6-noded ordinary triangular element.

If there are three singularities of orders $\lambda_1 - 1$, $\lambda_2 - 1$ and $\lambda_3 - 1$, one at a time, at the three corner nodes, we can write three sets of singular shape functions using eq. (12) repeatedly. The shape functions corresponding to the simultaneous occurrence of the three singularities are obtained by combining these three sets as follows.

$$\begin{aligned}
N_{1s} &= W_1\{1 - (1 - N_1)^{\lambda_1}\} + W_2\{N_1(1 - N_2)^{\lambda_2 - 1}\} + W_3\{N_1(1 - N_3)^{\lambda_3 - 1}\} \\
N_{2s} &= W_2\{1 - (1 - N_2)^{\lambda_2}\} + W_1\{N_2(1 - N_1)^{\lambda_1 - 1}\} + W_3\{N_2(1 - N_3)^{\lambda_3 - 1}\} \\
N_{3s} &= W_3\{1 - (1 - N_3)^{\lambda_3}\} + W_2\{N_3(1 - N_2)^{\lambda_2 - 1}\} + W_1\{N_3(1 - N_1)^{\lambda_1 - 1}\} \\
N_{4s} &= W_1\{N_4(1 - N_1)^{\lambda_1 - 1}\} + W_2\{N_4(1 - N_2)^{\lambda_2 - 1}\} + W_3\{N_4(1 - N_3)^{\lambda_3 - 1}\} \\
N_{5s} &= W_1\{N_5(1 - N_1)^{\lambda_1 - 1}\} + W_2\{N_5(1 - N_2)^{\lambda_2 - 1}\} + W_3\{N_5(1 - N_3)^{\lambda_3 - 1}\} \\
N_{6s} &= W_1\{N_6(1 - N_1)^{\lambda_1 - 1}\} + W_2\{N_6(1 - N_2)^{\lambda_2 - 1}\} + W_3\{N_6(1 - N_3)^{\lambda_3 - 1}\}
\end{aligned} \tag{13}$$

where W_1, W_2 and W_3 are appropriate weight functions. It is observed that, to satisfy the condition $N_{is} = 1$ at the ith node and the rigid body mode, i.e. $\Sigma N_{is} = 1$, the three weights should be such that

$$W_1 + W_2 + W_3 = 1.0. \tag{14}$$

If the element displacement field is written using the above shape functions (eq. 13), i.e.

$$u = \sum N_i u_i \quad \text{and} \quad v = \sum N_i v_i, \tag{15}$$

we obtain an element which has the singularities of orders $\lambda_1 - 1$, $\lambda_2 - 1$ and $\lambda_3 - 1$ at its three corner nodes 1, 2 and 3 respectively. The element meets the rigid body mode since $\Sigma N_{is} = 1$. The element is called here multiple singular points triangular element (MSPT).

Equation (14) indicates an infinite number of possibilities. The simplest possible solution is $W_1 = W_2 = W_3 = 1/3$. Equation (12) is the special case of eq. (13), because $W_1 = 1$ and $W_2 = W_3 = 0$. Another convenient combination is that $W_1 = L_1$, $W_2 = L_2$ and $W_3 = L_3$. When constant weights are used, the element displacement model does not have a linear term. This problem is obviated when these variable weights are employed. For all case studies reported in this paper, we have used these variable weights.

To obtain an element with two variable order singularities, it is just necessary to substitute, for example, $\lambda_3 = 1$ in eq. (13). This is the first degenerate form of the MSPT. The shape functions for one singular point element can be obtained by substituting, for example, $\lambda_3 = 1$ and $\lambda_2 = 1$ in eq. (13). This is the second degenerate form of the MSPT. If the MSPT element is used in

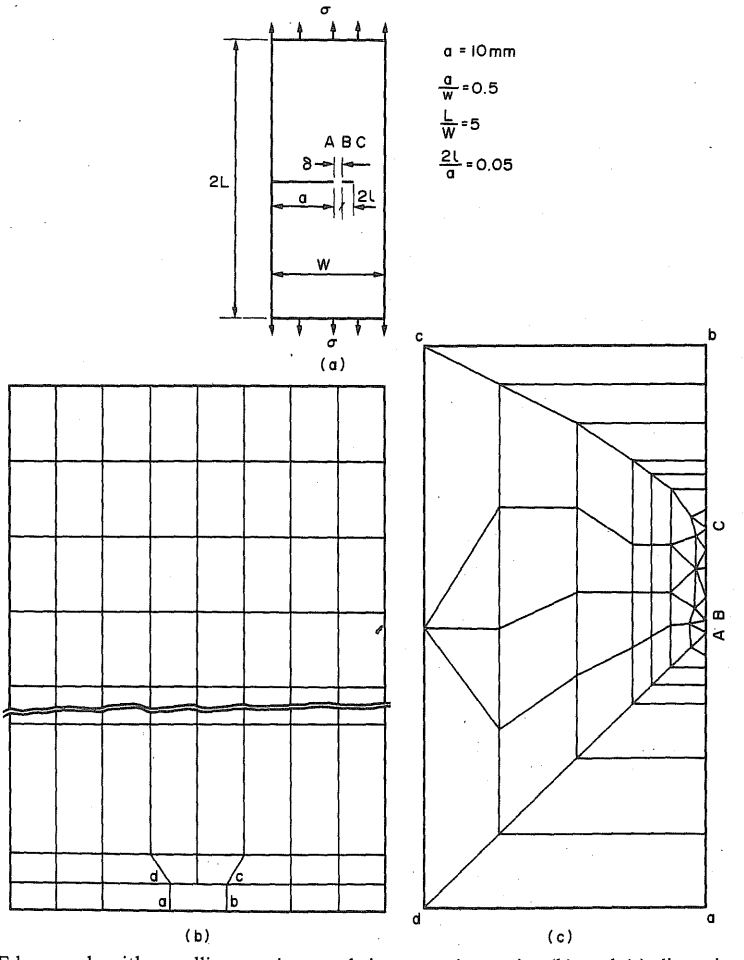

Fig. 2. (a) Edge crack with a collinear microcrack in a tenstion strip; (b) and (c) discretisation details.

conjunction with its first and second degenerate forms, interelement compatibility is obtained. These elements have been implemented in a 2-D displacement based finite element code CRACK2D[6].

CRACK–MICROCRACK INTERACTIONS

Microcracks can appear in the process zone ahead of a main crack in many situations. The microcrack can significantly alter the stress intensity factor at the main crack tip. An evaluation of the interaction effect is very important. There are some results available in the literature, which are mainly based on analytical techniques. We present results for two cases which have been examined by the finite element method. The MSPT and its two degenerate forms have been used for the purpose.

The first case is shown in Fig. 2(a). The study has been done for various ratios between the microcrack position (δ) and its length ($2l$). The plate was discretised by using 218 nodes and 106 elements. The element arrangement near, and away, from the microcrack are shown in Fig. 2(b) and (c) respectively. One 6-noded two singular points element has been used to cover the distance between the tips of the main crack and the neighbouring tip of the microcrack. The other singular elements are the 6-noded one singular point elements, which is the second degenerate form of the MSPT element. By this arrangement of elements we have ensured the interelement compatibility along all the element edges. To vary $\delta/2l$ ratio, the distance AB was kept constant and BC was varied by shifting the location of point C. A range of 0.075 to 0.3 was considered for $\delta/2l$. The stress intensity factor was calculated by using the method of crack closure integral[7]. Figure 3 shows the variation of K_I/K_{I0}, where K_{I0} is the main crack tip SIF in the absence of the microcrack. The variations reported by Kachanov[8–9] are included in this figure.

The second problem was on the interaction of the main crack with two stacked parallel microcracks (Fig. 4a). Results have been obtained for different ratios between the semi-stack height (h) and the microcrack length (l). Half of the domain was discretised because of the symmetry (Fig. 4(a) and (b)). There are 347 nodes and 104 elements in the discretisation. We have employed the 6-noded three singular points element (MSPT) along with its two degenerate forms. The SIF at the main crack tip was again calculated through the method of crack closure integral[7]. The variation of K_I/K_{I0}, where K_{I0} is the SIF in the absence of the microcracks, where h/l is shown in Fig. 5. The results due to Kachanov[6] are also shown in this figure.

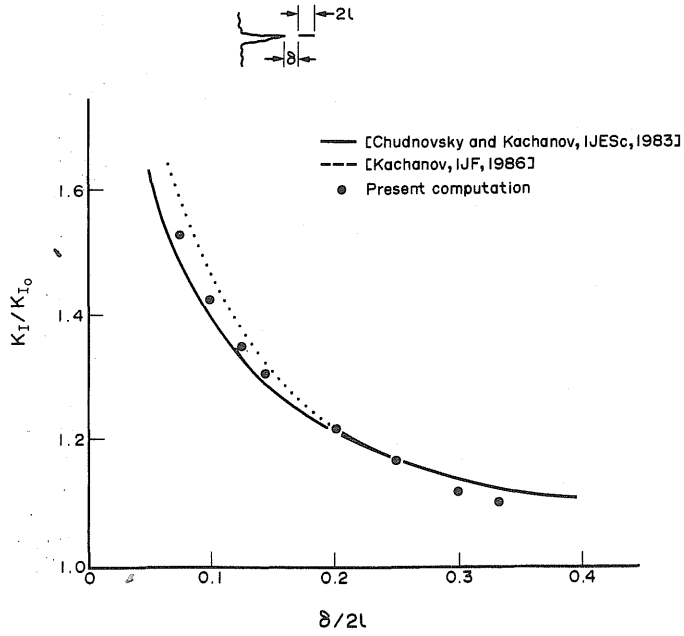

Fig. 3. Comparison of variation of K_I/K_{I0} with ratio ($\delta/2l$) between microcrack position and its length in the edge crack problem.

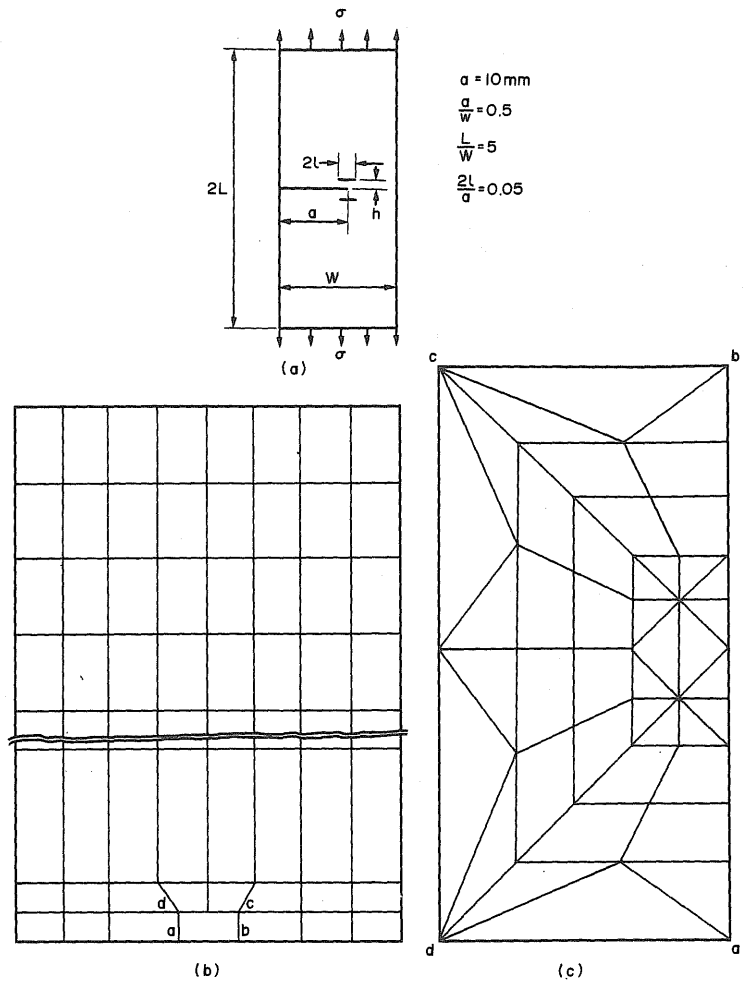

Fig. 4. (a) Single edge crack with two stacked microcracks in a tension strip; (b) and (c) discretisation details.

ANALYSIS OF DOUBLY KINKED CRACK

Very complex zig-zag cracks may come up due to stress corrosion cracking. We consider here a doubly kinked crack. At every knee point there is a singularity, whose order depends on the included angle. At the tip, there is a square root singularity. If the lengths of the kinks (AD and BC) are small, the three singularities (at A, B and C) can interact. The 3-noded two singular points elements along with its degenerate forms have been used in the analysis. The main crack is an edge crack in a long tension strip as shown in Fig. 6(a). The first kink AB, which has a length of 4% of the main crack (OA), makes an angle of 45° with OA. The second kink (BC) makes an angle θ with AB. The angle θ was varied between $-90°$ and $+90°$. The discretisation is shown in Figs 6(b) and (c). In all 180 nodes and 170 elements have been used in the discretisation. Two loadings were analysed. In the first case the plate was assumed to be under uniform tension. The stress intensity factors were calculated by comparing the net opening and sliding displacements[10]. The mode I and mode II SIFs at the tip C have been plotted for different values of θ in nondimensional form in Fig. 7. In the second case two collinear forces were applied on the main crack edges at an angle β. The β was varied from 0° to 90° in steps of 30°. The SIFs have been plotted in nondimensional form for different values of θ and β in Figs 8(a) and (b).

DISCUSSION AND CONCLUSION

The case studies presented here show the usefulness of the multiple singular points elements in analysing the interacting singularities in fracture mechanics.

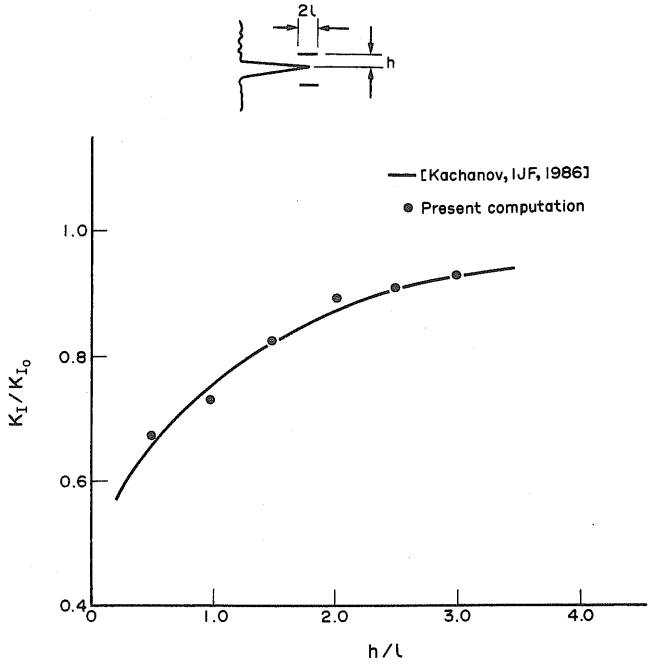

Fig. 5. Comparison of variation of K_I/K_{IO} with ratio (h/l) between semi-stack spacing and microcrack length.

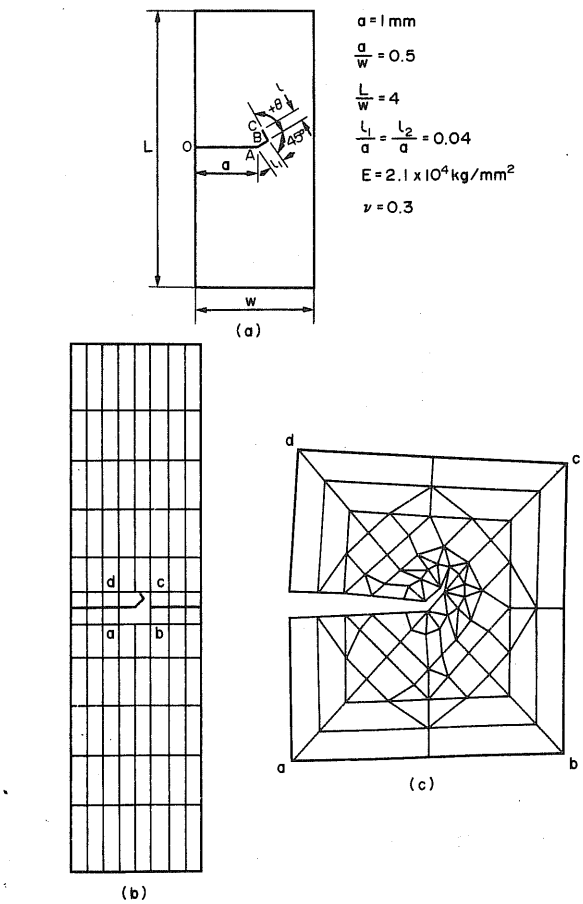

Fig. 6. (a) Single edge double kinked crack in a tension strip; (b) and (c) discretisation details.

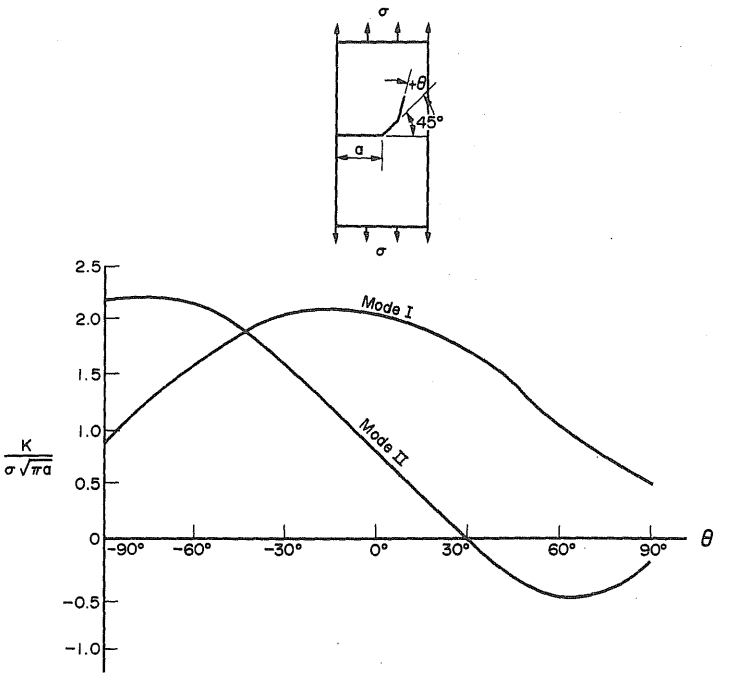

Fig. 7. Variation of mode I and mode II SIF for different orientation of the second kink under remote tension loading.

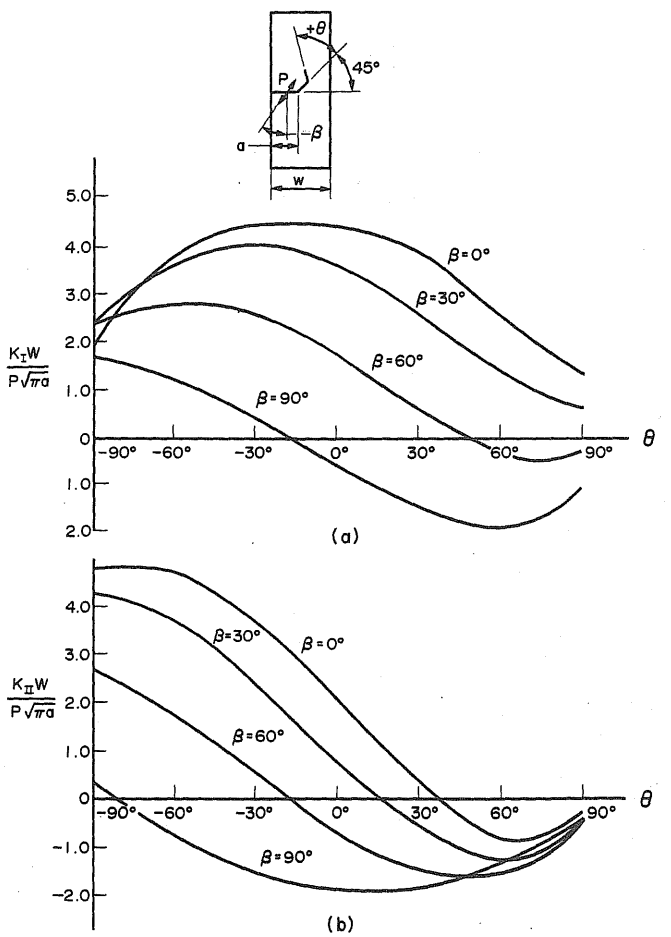

Fig. 8. Variation of SIF for different orientation of the second kink and loading directions in the case of crack edge point loading; (a) mode I variation; (b) mode II variation.

In both the examples on crack–microcrack interactions, the computed results are in good agreement with the analytical solutions. In the first case our results lie in between the values quoted in refs [8] and [9]. In the second case the difference with the values of ref. [8] is less than 5%. The study of doubly kinked cracks by the finite element method is the first of its kind and no comparison has been possible.

The numerical results presented in Figs 2–8 indicate the following. In the case of the first example, the problem of collinear cracks, as the size of the microcrack reduces with respect to its distance from main crack, the effect of its presence becomes negligible at the neighbouring main crack tip. In the second example, the stacked microcrack problem, there is a shielding at the main crack tip so long as the normal distance between the main crack and the microcrack is small. The shielding almost vanishes as the distance increases beyond about three times the semi-microcrack length. In the last example, the doubly kinked crack under remote tension (Fig. 7), the mode I SIF at the second kink tip generally decreases as this kink becomes more and more off the first kink. This is a short of shielding. The mode II SIF increases as θ varies from 0° to $-90°$ (Fig. 7), but remains below its 0° value as θ varies between 0° and $+90°$. A similar trend is observed when crack edge point loading makes an angle 90° ($\beta = 0°$) with the axis of the main crack (Fig. 8).

REFERENCES

[1] M. L. Williams, Stress singularities resulting from various boundary conditions in angular corners of plates in extension. *J. appl. Mech.* **19,** 526–528 (1952).

[2] B. K. Dutta, S. K. Maiti and A. Kakodkar, Development and application of two singular points finite elements. *Int. J. numer. Meth. Engng* **28,** 1449–1460 (1989).

[3] B. K. Dutta, S. K. Maiti and A. Kakodkar, On the use of one point and two points singularity elements in the analysis of kinked cracks. *Int. J. numer. Meth. Engng* **29,** 1487–1499 (1990).

[4] B. K. Dutta, S. K. Maiti and A. Kakodkar, A 6-noded triangular element to model up to three variable order singularities lying in close proximities. *Communications appl. numer. Meth.* (In press, 1991).

[5] D. M. Tracey and T. S. Cook, Analysis of power type singularities using finite elements. *Int. J. numer. Meth. Engng* **11,** 1225–1233 (1977).

[6] B. K. Dutta, A. Kakodkar, S. K. Maiti, Development of a computer code CRACK for elastic and elastoplastic fracture mechanics analysis of 2-D structure by finite element technique. *BARC*–1346 (1986).

[7] G. R. Irwin, Fracture I, Handbuch der Physik VI (Edited by S. Flugge), pp. 558–590. Springer, Berlin (1958).

[8] M. Kachanov, On crack–microcrack interactions. *Int. J. Fracture* **30,** R65-R72 (1986).

[9] A. Chudnovsky and M. Kachanov, Interaction of a crack with a field of microcracks. *Int. J. Engng Sci.* **21,** 1009–1018 (1983).

[10] G. E. Blandford, A. R. Ingraffea and J. A. Liggett, Two-dimensional stress intensity factor computation using the boundary element method. *Int. J. numer. Meth. Engng* **17,** 387–404 (1981).

(*Received* 11 *December* 1989)